Table 1 List of state vectors

	Single balance	Coupled balance
Human subject	$\Delta x_H = (\Delta x_H; \Delta \underline{x}_H)^T$ where $\Delta x_H := x_H^t - x_H^c$	$\Delta X_H = (\Delta X_H; \Delta \underline{X}_H)^T$ where $\Delta X_H := X^t - X_H^c$
Artificial controller	$\Delta x_A = (\Delta x_A; \Delta \underline{x}_A)^T$ where $\Delta x_A := x_A^t - x_A^c$	$\Delta X_A = (\Delta X_A; \Delta \underline{X}_A)^T$ where $\Delta X_A := X^t + l - X_A^c$
Total dynamics		$\Delta X = (\Delta X_H; \Delta \underline{X}_H; \Delta X_A; \Delta \underline{X}_A)^T$

2.2 Human Control

We also develop a balance control system with a single human subject as schematically shown in Fig. 4. Watching the computer screen displaying a simulated motion of the linearized inverted pendulum, the subject manipulates the displacement of cart x_H^c by mice. In this system, the subject can perform a balancing task, manipulating the cart x_H^c to make it track the target repelling from the cart. To achieve this, we replace eq.(3b) with the human manipulation as follows.

$$\ddot{x}_H^t + \gamma \underline{x}_H^t - \alpha \Delta x_H = 0; \quad (4a)$$

$$x_H^c := (\text{manipulation by a human subject}); \quad (4b)$$

$$\Delta x_H := x_H^t - x_H^c \quad (4c)$$

where Δx_H is the balancing error and x_H^c is the human manipulation measured by the mice device. All the parameters except ν, τ and β are the same values as were in Section 2.1. We set initial values of the model to $[x_H^t; \underline{x}_H^t; x_H^c]^T = [0{:}1; 0; 0]^T$. This means that the initial balancing error is set to $\Delta x_H = 0{:}1$. The movement x_H^c is measured and substituted into eq.(4b) with a sampling rate of 20Hz, while the balancing image on the screen is animated at the same rate. In what follows, we numerically approximate a velocity $\underline{x}_i$ of a measured time series $x_i := x(t_0 + i\Delta t)$ as the following backward di erence:

$$\underline{x}_i \approx \frac{x_{i+1} - x_i}{\Delta t} \quad (i = 1; 2; \cdots) \quad (5)$$

where sampling time is $\Delta t = 0{:}05$s. The method of numerical integrations of eq. (4) is the same as was in Section 2.1.

Based on this system, we conduct the experiment to measure the time series of Δx_H and $\Delta \underline{x}_H$ for 10 subjects who were healthy males in their early twenties.

The subjects were first instructed in how to operate of the measurement system, the number of trials to be performed, the initial configuration of the target model, and the time interval of trial.

In the actual trial, they began the operation upon hearing a signal and attempted to maintain the balance for 60s. If a target or cart left the screen in less than 60s, the trial was repeated. After completing the 10 trials, the measurements were over.

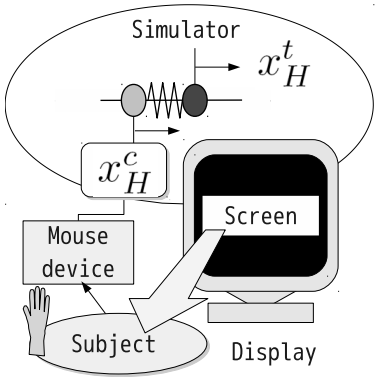

Fig. 4 Single balance control system with a human subject

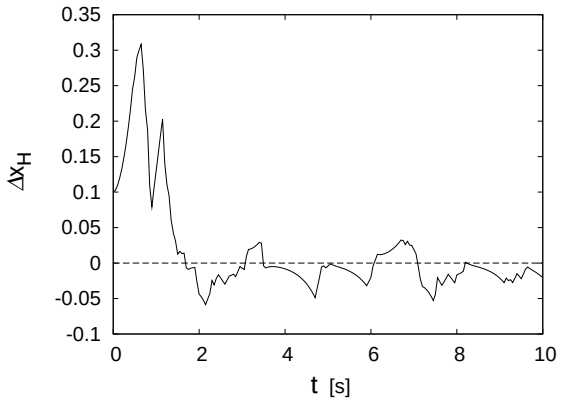

Fig. 5 Time series of the balancing error $\Delta x_H(t)$

Fig. 5 shows a typical time series of the balancing error $\Delta x_H(t)$ produced by a human subject. It appears that amplitudes of the balancing error $\Delta x_H(t)$ rapidly decreases in about 2s to drop into some stationary state fluctuated around $\Delta x_H(t) = 0$ with small amplitudes.

3. Coupled Balancing Tasks

The main interest of this paper is to combine the artificial and human balance control systems discussed in Chapter 2 into a coupled balance control system with the human subject and the artificial controller as shown in Fig. 6. In this coupled balance, one of the carts is controlled by the artificial controller as was

$$\dot{\xi}(t) = J\big(x(t)\big)\xi(t); \quad \xi(0) = \xi_0 \tag{8}$$

where $J(x) = \partial f/\partial x$ is the Jacobian matrix of f along the orbit $x(t)$. Then, the largest Lyapunov exponent (LLE) of the dynamical system eq. (7) is defined by

$$\lambda(x) = \max_{\xi_0} \lim_{t \to \infty} \frac{1}{t} \ln \frac{\|\xi(t)\|}{\|\xi(0)\|} \tag{9}$$

where $\|\cdots\|$ is a norm of vectors. In general, the trajectory $x(t)$ is stable for $\lambda < 0$, unstable for $\lambda > 0$, and neutrally stable for $\lambda = 0$.

It is noteworthy that the LLE is similar to the maximal real part of the eigenvalue of linear systems in the sense of evaluating dynamic stabilities while their target of evaluation is different. The maximal real part of the eigenvalue of linear systems represents stability of a corresponding equilibrium point. In contrast, the LLE represents local stability of solution trajectories.

When the system equation in eq. (7) is explicitly known, one can calculate the LLE $\lambda(x)$ by solving eq. (8) along with eq. (7) numerically. Therefore, in this way, the LLE of the single artificial balance control system, $\lambda(\Delta x_A)$, can be obtained.

On the contrary, another approach is required for the balance control systems including human subjects because their system equation is not explicitly known. For this purpose, we employ an effective method of estimating the LLE from physical time series proposed by Sano and Sawada[11]. In this case, a time series $x_j = x\big(t_0 + (j-1)\Delta t\big)$ of the target system is assumed to be known where Δt is a sampling time of measurement. Then, consider a small ball of radius ϵ centred at the orbit point x_j and find any set of N points $\{x_{k_i}\}_{i=1}^{N}$ included in this ball and define the displacement vectors:

$$y^i := x_{k_i} - x_j; \quad (i = 1,2,\cdots,N). \tag{10}$$

After the evolution of a time interval $m\Delta t$, the orbital point x_j will proceed to x_{k_i+m} and neighboring points $\{x_{k_i}\}_{i=1}^{N}$ to $\{x_{k_i+m}\}_{i=1}^{N}$. The displacement vector y^i is thereby mapped to

$$z^i := x_{k_i+m} - x_{j+m}; \quad (i = 1,2,\cdots,N). \tag{11}$$

If the radius ϵ is sufficiently small, the evolution of y^i to z^i can be represented by

$$z^i = A_j y^i; \quad A_j V = C; \quad (V)_{kl} = \frac{1}{N}\sum_{i=1}^{N} (y^i)_k (y^i)_l;$$
$$(C)_{kl} = \frac{1}{N}\sum_{i=1}^{N} (z^i)_k (y^i)_l \tag{12}$$

where $(\cdots)_k$, $(\cdots)_{kl}$ denotes the k component of vector and the (k,l) component of matrix respectively. Finally, using the estimated matrix A_j in eq. (12), we can define the LLE of the time series x_j as

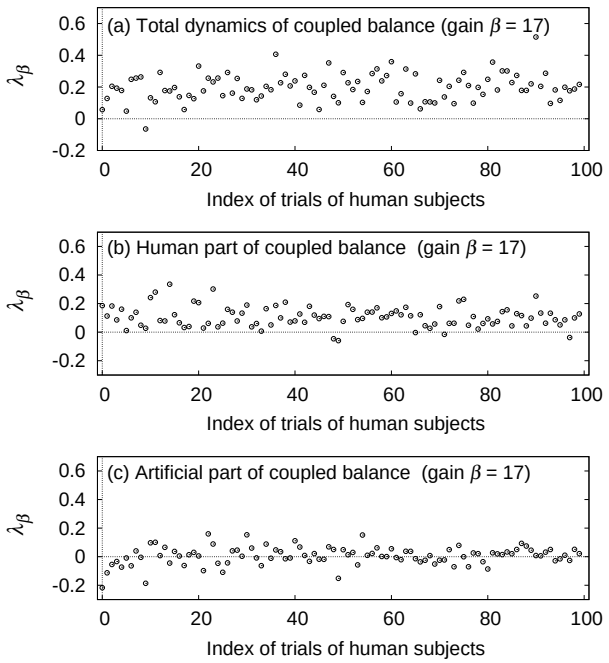

Fig. 9 LLE of coupled balance for $\beta = 17$

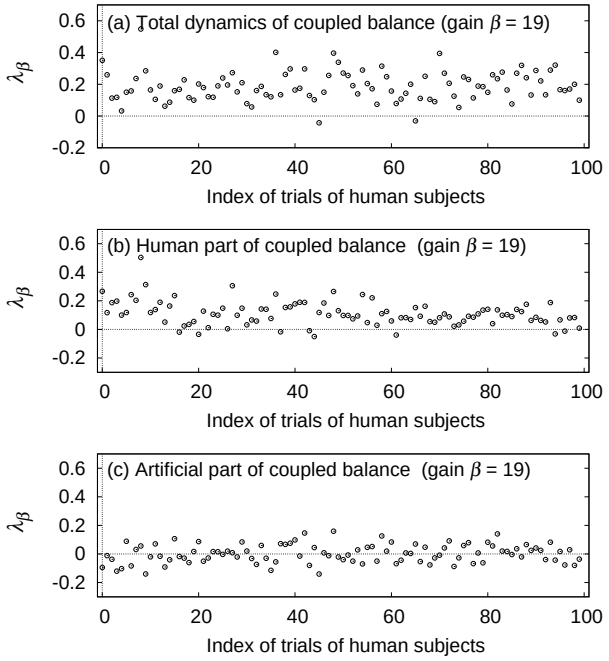

Fig. 10 LLE of coupled balance for $\beta = 19$

$$\lambda(x_j) = \max_{u} \lim_{n \to \infty} \frac{1}{n\Delta t} \sum_{j=1}^{n} \ln \frac{\|A_j u\|}{\|u\|} \tag{13}$$

where u is a tangent vector at x_j. In the following, we choose $\epsilon = 0.05$, $N = 10$, $m = 200$ and $\Delta t = 0.05$s. In this way, we can obtain the LLE such as $\lambda(\Delta x_H)$ for the single balance with a human subject, $\lambda(\Delta X)$ for the coupled balance with human subject and the artificial controller. In the same way, it is also possible to obtain the sub-LLE of the human part $\lambda(\Delta X_H)$ and the artificial part $\lambda(\Delta X_A)$ of the coupled balance.

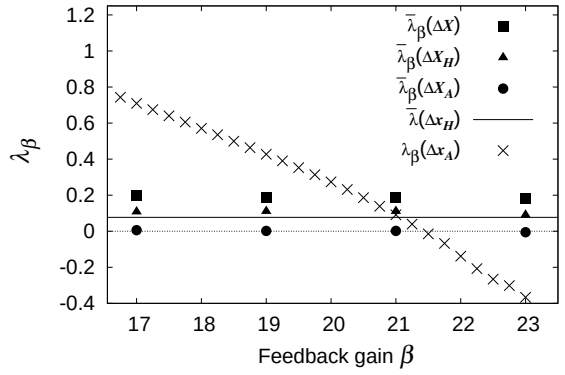

Fig. 14 Mean LLEs of the experiments

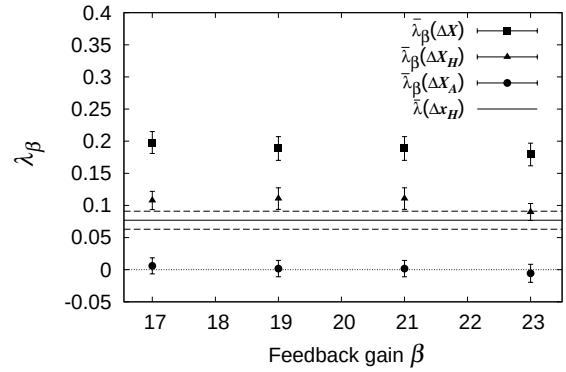

Fig. 15 Mean LLEs of the experiments with 95% confidence intervals

words, it seems that the human part may adjust itself to make the total stability of the coupled balance nearly constant. This feature can also be found in Figs. 7, 8 where the different values of β does not cause big changes in the time responses of the coupled balance.

4.3 Sub-LLE of the human part

The triangles in Fig. 14 represent the mean sub-LLE, $\bar{\lambda}\ (\Delta X_H)$, of the human part of the coupled balance as functions of the feedback gain β, and the solid line in Fig. 14 represent the mean LLE, $\bar{\lambda}(\Delta x_H)$ of the single human balance. The errorbars plotted along with the triangles in Fig. 15 represent 95% confidence intervals of the mean values $\bar{\lambda}\ (\Delta X_H)$, and the dashed lines around the solid line in Fig. 15 represent that of the mean value $\bar{\lambda}(\Delta x_H)$.

It appears in Figs. 14, 15 that both $\bar{\lambda}\ (\Delta X_H)$ and $\bar{\lambda}\ (\Delta x_H)$ take nearly constant positive values around $\lambda \approx 0.1 > 0$, and that the balancing error of the human part ΔX_H exhibits the second largest fluctuation of the trajectory among three types of balancing errors of the coupled balance listed in Table 1. This means that the human balancing dynamics exhibits nearly constant instability independently of existence of the coupling and of the feedback gain of the artificial part.

4.4 Sub-LLE of the artificial part

The circles in Fig. 14 represent the mean sub-LLE, $\bar{\lambda}\ (\Delta X_A)$, of the artificial part of coupled balance, and the cross marks in Fig. 14 represent LLE, $\lambda\ (\Delta x_A)$, of the single artificial balance as a function of β. The errorbars plotted along with the circles in Fig. 15 represent 95% confidence intervals of the mean values $\bar{\lambda}\ (\Delta X_A)$.

As was mentioned in Section 4.2 for the single balance, the LLE, $\lambda\ (\Delta x_A)$, is a monotonically decreasing function of β, showing that the stability of the single artificial balancing depends on the feedback gain β.

In contrast, it is clear from the result on $\bar{\lambda}\ (\Delta X_A)$ that the artificial part of the coupled balance maintains nearly a constant value about 0 of the LLE, and that the balancing error of the artificial part ΔX_A exhibits the smallest fluctuation of the trajectory among three types of balancing errors of the coupled balance listed in Table 1.

As was mentioned in Section 4.2, since β represents the feedback gain of the artificial part (not of the human part), the result implies that nearly constant neutral stability of the artificial part of the coupled balance in Figs. 14, 15 is possibly produced by the human part. In other words, it seems that the human subjects in this study try to make the artificial controller minimally or neutrally stable.

It should be noted that the property of human described above, seeking the neutrally stable artificial partners, seems to be hardly obtainable from the conventional design principles of control systems engineering, in other words, it may be brought about by human specific nature.

5. Conclusion

We have experimentally studied how human subjects tune their control properties when playing balancing tasks in cooperation with a given artificial controller having several different specifications of feedback gain β. To this end, we conducted the experiment to measure the time responses of the balancing errors in the single human balance, in the single artificial balance, and in the coupled balance between a human subject and an artificial controller. We then calculated the largest Lyapunov exponent (LLE) of the balancing errors in order to evaluate their stabilities and obtained the following results.

- The stability of the single artificial balance monotonically depends on the feedback gain β.
- In contrast, the total dynamics of the coupled balance between the human subject and the artificial controller exhibits instability nearly constant with β.
- The human subject always exhibits nearly constant instability with β in both cases of the single balance and the coupled balance.
- The artificial part in the coupled balance maintains neutrally stable state independent of β.